IEEE Access
Multidisciplinary | Rapid Review | Open Access Journal

Received October 6, 2019, accepted October 22, 2019, date of publication October 29, 2019, date of current version November 8, 2019.

Digital Object Identifier 10.1109/ACCESS.2019.2950012

Bio-Based Polycationic Polyurethane as an Ion-Selective Membrane for Nitrate Tapered Optical Fiber Sensors

ATIQAH YUSOFF[1], NUR HIDAYAH AZEMAN[1], (Member, IEEE), MUHAMMAD FAIZAL MOHAMED KASSIM[2], NADHRATUN NAIIM MOBARAK[2], KHAIRIAH HAJI BADRI[2], MOHD ADZIR MAHDI[3], (Senior Member, IEEE), MOHD SUKOR SU'AIT[4], AND AHMAD ASHRIF A. BAKAR[1], (Senior Member, IEEE)

[1]Photonics Technology Laboratory, Center of Advanced Electronic and Communication Engineering, Faculty of Engineering and Built Environment, Universiti Kebangsaan Malaysia (UKM), Bangi 43600, Malaysia
[2]School of Chemical Sciences and Food Technology, Faculty of Science and Technology, Universiti Kebangsaan Malaysia (UKM), Bangi 43600, Malaysia
[3]Wireless and Photonics Network Research Center, Faculty of Engineering, Universiti Putra Malaysia (UPM), Serdang 43400, Malaysia
[4]Solar Energy Research Institute, Universiti Kebangsaan Malaysia (UKM), Bangi 43600, Malaysia

Corresponding authors: Nur Hidayah Azeman (nhidayah.az@ukm.edu.my); Mohd Sukor Su'ait (mohdsukor@ukm.edu.my); and Ahmad Ashrif A. Bakar (ashrif@ukm.edu.my)

This work was supported in part by the Universiti Kebangsaan Malaysia through the Human Capital under Grant MI-2018-018, in part by the Research University under Grant GUP-2017-30, and in part by the Ministry of Education Malaysia under the Fundamental Research Grant Scheme under GrantFRGS/1/2018/TK04/UKM/02/6.

ABSTRACT A novel bio-based polycationic polyurethane as an ion-selective membrane for nitrate sensing was successfully developed. In this work, the intermolecular interactions at active polymeric sites play a primary role in selective nitrate-ion detection. From the experiment, FTIR shows a significant shift from 1543 cm^{-1} to 1548 cm^{-1} in N-H bending, indicating that intermolecular interactions occur between the polycationic polyurethane and nitrate. AFM shows that the surface roughness of the polycationic polyurethane decreases from 95.7 nm to 12.2 nm after immersion in nitrate solution. Meanwhile, FESEM images show that the bright area, which represents the hard segment of polycationic polyurethane, decreases after immersion, indicating that the nitrate is interacting with the hard segment of the polycationic polyurethane via intermolecular interaction. Furthermore, EIS shows that the conductivity increases from 2.84×10^{-11} to 5.34×10^{-11} S cm^{-1} after ion exchange occurs between the iodide and nitrate on the polycationic polyurethane. To assess the sensing performance, the sensor probe is fabricated by coating the polycationic polyurethane thin film on the tapered region of an optical fiber. Rapid detection, good repeatability, and a sensitivity of $5.94 \times 10^{-2} \mu$W/ppm are obtained for nitrate detection using the above bio-based-sensing material. The selectivity study also shows that the sensing material possesses high affinity toward the nitrate ion.

INDEX TERMS Optical fiber sensor, chemical sensor, ion-selective membrane, nitrate sensing, polyurethane.

I. INTRODUCTION

Nitrate is an ionized form of nitrogen and an important nutrient for all photosynthetic organisms. Because of their involvement in the biogeochemical cycle in water reservoirs, nitrate sensing in water is vital for monitoring and sustaining water quality conditions [1], [2]. However, the excessive consumption of nitrate by humans may lead to methemoglobinemia disease. Furthermore, excessive amounts of nitrate can also cause harmful impacts toward the environment, such as eutrophication, algal blooms and the death of aquatic life [3].

Conventionally, nitrate detection is carried out in the laboratory, where the water sample is collected and preserved under a specific condition prior to analysis. Under certain conditions, an additional pretreatment process is required before the analysis [4]. The water sample is then analyzed using sophisticated techniques such as atomic absorption/emission spectroscopy (AAS/AES), chromatography,

The associate editor coordinating the review of this manuscript and approving it for publication was Sukhdev Roy.

and inductively coupled plasma-mass spectrometry (ICP-MS) [5], [6]. Although these techniques have been practiced for many years, they do have limitations; the above techniques are tedious, nonportable and may lead to sample contamination during preservation. Thus, many researchers have opted to explore alternative ways to improve the existing techniques.

Recently, the development of an optical fiber sensor technique for nitrate detection has gained interest among researchers. This technique can be applied in situ and is straightforward, cost effective and resistant to environmental electromagnetic interference [7]. Lalasangi and coworkers [8] reported utilizing an etched fiber Bragg grating (FBG) as a sensing probe to observe the wavelength shift, which corresponds to the variation of nitrate concentrations and resulted in a sensitivity of 1.322×10^{-3} nm/ppm. Later, Camas-Anzueto *et al*. [1] claimed that by integrating a sensing material (lophine(2,4,5-triphenylimidazole)) with an optical fiber, nitrate could be detected as low as 1 ppm with a good response and recovery time of 20 ms and 40 ms, respectively. Meanwhile, Moo *et al*. (2016) [7] developed a simultaneous measurement procedure using an ultraviolet optical fiber sensor without a coating for detection of nitrate that ranges from 0 to 50 ppm with a detection limit of 0.0017 ppm.

The performance of the optical fiber sensor can be further improved by modifying the geometrical structure of the optical fiber. Such modifications can be carried out by tapering the optical fiber, leading to a high interaction between the light-sensing material and the chemical analytes [9], [10]. The tapering modification for the optical fiber is integrated with a sensing material in such a way that the optical fiber sensor is both sensitive and selective towards the target chemical analytes.

Bio-based polyurethane is a polymer derived from vegetable oils and can be produced via the polymerization of polyols and isocyanates. The presence of polyols and isocyanates in a polymeric chain structure provide the soft and hard segment features of this material. The hard segment of polyurethane acts as a supporting pillar and interconnects throughout the soft phase segment, therefore contributing to the mechanical strength of the polymer [11] and preserving the stability of the material on the sensor surface [12]. Recently, polyurethane has been modified physically by introducing fillers to improve its properties for pressure [13], strain [14] and piezoresistive [15] sensors. Another way to modify polyurethane is through chemical modification by introducing various functional groups in its structure. One of the methods is by introducing a propyl functional group via an alkylation reaction to the polyurethane structure; hence, a comb-like polymer with a positive charge in its structure is produced. The positive charge of the molecule is able to interact and form bonds with the negatively-charged analyte via electrostatic interaction.

In this work, we synthesized a novel bio-based polycationic polyurethane as a sensing material for nitrate detection. The polycationic polyurethane was characterized, and the physicochemical properties of this material were studied prior to integration with a tapered optical fiber. To assess the sensor performance, various ranges of nitrate concentrations were used. The sensitivity, response time, repeatability and selectivity of the sensor were evaluated. By incorporating a bio-based sensing material with an optical fiber, a more environmentally friendly sensing system can be developed for nitrate detection with good sensitivity and selectivity. To the best of our knowledge, the incorporation of a polycationic polyurethane as the sensing material with a tapered optical fiber for nitrate sensing has never been reported in the literature.

II. EXPERIMENTAL SECTION

A. MATERIALS

Palm kernel oil-based monoester-OH (PKO-p) was prepared following the method developed by Badri *et al*. (2000) [16]. The 2,4-methylene diphenyldiisocynate (MDI) was obtained from Cosmo Polyurethane. The acetone was purchased from SYSTERM ChemAR. The iodopropane (99%) was purchased from Sigma Aldrich.

B. PREPARATION OF POLYCATIONIC POLYURETHANE

An amount of palm kernel oil-based monoester-OH (PKO-p) and 2,4-methylene diphenyl diisocynate (2,4-MDI) were dissolved in acetone for several hours in separate vials [13], [17]. After that, the MDI solution was mixed with PKO-p producing a homogeneous solution. Then, the iodopropane solution was added under continuous stirring for another several minutes under a nitrogen gas atmosphere. Samples were kept under a nitrogen atmosphere until use.

C. PHYSICOCHEMICAL PROPERTIES AND SURFACE MORPHOLOGY OF POLYCATIONIC POLYURETHANE

To study the physicochemical properties and surface morphology of the sensing material, polycationic polyurethane was deposited on glass slides with dimensions of 2.5×3.0 cm by using a dip-coating technique. The prepared glass slides were then coated with polycationic polyurethane by using a dip-coating technique and the aid of a programmable dip-coater machine (PTL-MMB01, MTI Corp.). The speed of the dip-coater machine varied from 10 mm/min to 200 mm/min. The coated glass slides were characterized using a UV-Vis spectrophotometer to optimize the thickness of the thin film and soaking time based on the optimum absorbance and reflectance values of the material. The thickness of the thin film was measured by using a profilometer machine (DektakXT, BRUKER). The optimized film thickness obtained from this analysis was further used as the coating thickness for the tapered optical fiber. The topography and surface morphology of the sensing material was characterized using a Nanosurf Easyscan2 atomic force microscope (AFM) and a LEVO 1450VP field emission scanning electron microscope (FESEM) with a magnification of 5000 $\times$ and 10,000 $\times$, respectively. The synthesized polycationic polyurethane was

also characterized using a Perkin Elmer Spectrum 400 Fourier transform infrared (FTIR) spectrometer ranging from 4000 to 650 cm^{-1} with a scanning resolution of 2 cm^{-1} and appropriate scan rates to observe the vibrational mode of functional groups. The electrical properties of the sensing material were characterized by an alternating current electrochemical impedance spectrometer (EIS, Princeton VERSASTAT4) equipped with a frequency resonance analyzer (FRA) at an applied frequency ranging from 1 MHz to 0.1 Hz and 10 mV. The 1.5 mm^2 rectangular-shaped polycationic polyurethane sample was sandwiched between two conductive glass electrodes. The EIS analysis was carried out at different concentrations in the range of 0.01 ppm to 8 ppm of nitrate solutions. All the electrical parameters were extracted from the Nyquist plots formed from the EIS measurements.

D. PREPARATION OF NITRATE SOLUTIONS

Nitrate solutions were prepared using dilution techniques. First, 30.61 mg of LiNO3 was diluted in 1 L of deionized water as a stock solution with a 100% concentration of nitrate ions. The stock solution was then diluted to 8 different nitrate solution concentrations in the range of 0 ppm to 30 ppm.

E. PREPARATION OF THE TAPERED OPTICAL FIBER

A multimode-type optical fiber was used throughout the study. In this work, the same parameters of tapered optical fiber were used as in our previous report [10]. Tapered-multimode optical fiber was prepared by using a Vytran GPX-3400 machine. A standard-grade optical fiber was heated using a filament heater while both sides of the fiber were simultaneously pulled, producing a smaller region in the middle of the fiber. In this work, a standard-grade optical fiber with a cladding/core size of 125 μm/62.5 μm was tapered to thin down the core/cladding waist diameter to 50 μm. The transition region and taper lengths were fixed at 5 mm and 3 cm, respectively. Prior to the sensor probe fabrication, the tapered region of the optical fiber was cleaved at a 90° at the fiber tip with a tapered-region length of 3.0 cm. Then, the fiber surface was cleaned using acetone prior to the sensing material coating. Figure 1 shows the schematic diagram of the tapered optical fiber structure used in this study.

F. FABRICATION OF THE SENSOR PROBE

The sensor probe was fabricated by coating the polycationic polyurethane on the tapered optical fiber surface by using a dip-coating technique. The coated region was dipped in the polycationic polyurethane solution for 10 minutes and dried for another 10 minutes at 90 °C. The dip-coating process was repeated twice to produce two layers of sensing material on the optical fiber surface using a dip-coater machine (PTL-MMB01, MTI Corp). The speed of the dip-coater machine was fixed at 200 mm/min. The thickness of the coating material on the tapered optical fiber surface was then characterized by using FESEM analysis.

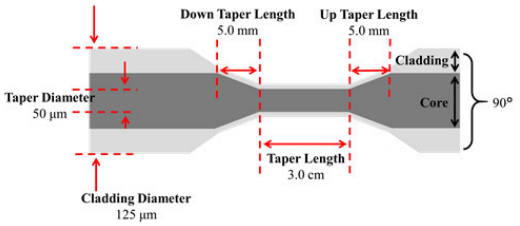

FIGURE 1. Schematic diagram of the tapered optical fiber structure.

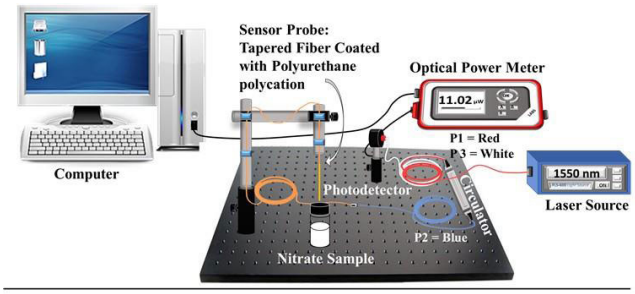

FIGURE 2. Experimental setup for detection of nitrate using the tapered optical fiber coated with polycationic polyurethane.

G. EXPERIMENTAL SETUP FOR NITRATE SENSING

Figure 2 shows the experimental setup for the nitrate sensor using a tapered optical fiber in a reflectance configuration. The tapered optical fiber coated with polycationic polyurethane was immersed in 8 different concentrations of nitrate solution from low to high. The wavelength used was 1550 nm with a modulated light source (FLS-130A, EXFO). An S122C Thorlabs photodetector was used to convert the optical signal to an electrical signal. An optical power meter (PM100D, Thorlabs) was used to measure the power output. The collected data from this analysis was used for the sensor performance evaluation.

III. RESULTS AND DISCUSSION

A. FOURIER TRANSFORM INFRARED SPECTROSCOPY (FTIR)

Figure 3 shows the FTIR spectra for polyurethane, polycationic polyurethane and polycationic polyurethane-nitrate. After the polymerization of polyurethane (blue line), the appearance of the peak at 3330 cm^{-1} represents the stretching mode of amine (N-H) and verifies the presence of secondary amides (-NHCO-) in the polymeric polyurethane structure [17]. Furthermore, the appearance of the peak at 1715 cm^{-1} represents the C = O stretching of the urethane functional group. Meanwhile, C-N is attributed to peak at 1310 cm^{-1} [17].

The addition of iodopropane in the polyurethane (red line) causes the significant shift of the carbamide group (C-N bending) from 1310 cm^{-1} to 1312 cm^{-1} and validates the presence of a propyl group attached to an amide functional group, as shown in Figure 3 [18], [19]. A peak shift is also observed for N-H bending from 1541 cm^{-1} to 1543 cm^{-1}.

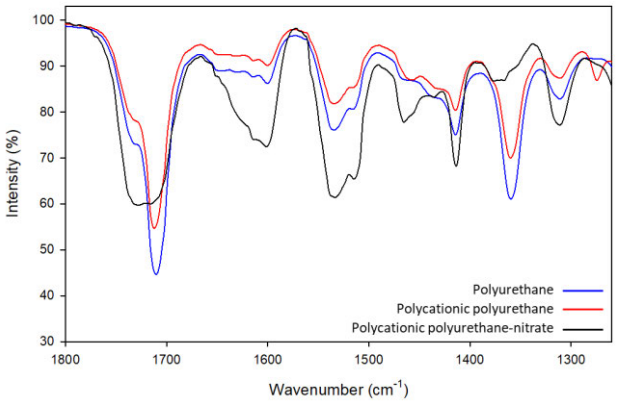

FIGURE 3. FTIR spectra for polyurethane, polycationic polyurethane and polycationic polyurethane-nitrate.

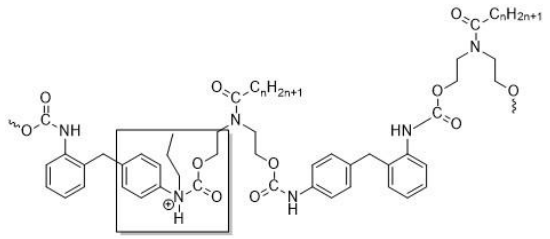

FIGURE 4. Structure of polycationic polyurethane.

No significant shift is observed for the carbonyl stretching (C = O) of the urethane functional group (from 1715 cm^{-1} to 1714 cm^{-1}). After the polycationic polyurethane is immersed in nitrate solution (black line), a significant shift is observed for N-H stretching (hydrogen bonded) from 3308 cm^{-1} to 3299 cm^{-1}, whereas the oxygen is shifted to a higher wavenumber, suggesting that there are possibilities that ion exchange occurred between the nitrate and iodide at the amide functional group. In addition, the wavenumber of the carbonyl group (C = O) is shifted to the right (1714 cm^{-1} to 1710 cm^{-1}), indicating the weakening of the intermolecular forces in the polyurethane chain structure [17]. The intermolecular interaction between the polycationic polyurethane and nitrate is verified by the shifting of N-H bending to a higher wavenumber from 1543 cm^{-1} to 1548 cm^{-1}.

Table 1 shows a summary of the respective functional groups and wavenumbers for polyurethane, polycationic polyurethane and polycationic polyurethane-nitrate. Moreover, Figures 4 and 5 exhibit the structure of polycationic polyurethane and the chemical interaction between the polycationic polyurethane with nitrate ions, respectively. Figure 5 shows that the nitrogen atom of the amide group in the polycationic polyurethane that bears a positive charge is able to interact with the negatively charged analyte through electrostatic interaction, hence making this material suitable for nitrate detection. The detailed mechanism of reaction is shown in the supplementary material, Figure S1.

B. ATOMIC FORCE MICROSCOPY (AFM)

Figure 6 shows the AFM topography of polycationic polyurethane and polycationic polyurethane after immersion

TABLE 1. Wavenumbers of functional groups in polyurethane, polycationic polyurethane and polycationic polyurethane-nitrate.

Functional Groups	Frequency Number (cm^{-1})		
	Polyurethane	Polycationic Polyurethane	Polycationic Polyurethane-Nitrate
N-H (Stretch)	3330	3308	3299
N-H (Bend)	1541	1543	1548
C=O	1715	1714	1710
C-N (Carbamide)	1310	1312	1311
C-H (Bend)	3301	2922	2924
$C-H_3$	1413	1413	1414

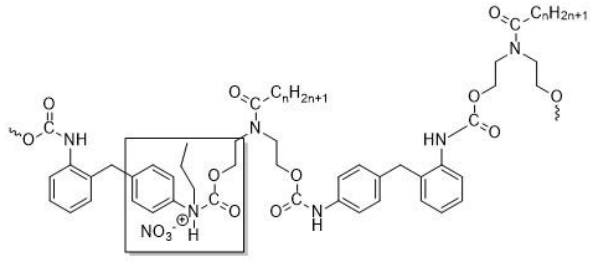

FIGURE 5. Structure of polycationic polyurethane-nitrate.

in a nitrate solution. The surface roughness calculated for polycationic polyurethane is 95.7 nm, showing that the overall topography of polycationic polyurethane is rough [20]. High surface roughness provides more adsorption sites for analyte attachment [21]. However, the surface roughness of polycationic polyurethane after immersion in nitrate is reduced to 12.2 nm. The declining surface roughness of the polycationic polyurethane after immersion in a nitrate solution verifies the occurrence of ion exchange between the iodide and nitrate ions, as observed in the FTIR analysis (Figure 3).

C. FIELD EMISSION SCANNING ELECTRON MICROSCOPY (FESEM)

Figure 7 shows the field emission scanning electron microscopy (FESEM) images for (a) polycationic polyurethane and (b) polycationic polyurethane immersed in a nitrate solution. The polycationic polyurethane possesses crystalline and amorphous phases contributed by the alignment of hard and soft segments, respectively. In Figure 7(a), the bright area representing the crystalline region associated with the hard segment of polycationic polyurethane dominates the cross-section of the thin membrane [20]. However, when polycationic polyurethane is immersed in nitrate solution, the bright area decreases and the dark area increases, indicating that the amorphous region increases. This phenomenon is confirmed by the disturbance in the intermolecular interaction observed in the FTIR analysis. It is believed that the existing physical crosslinking of polycationic polyurethane (hydrogen bond interaction between the hard and soft segments of polycationic polyurethane) are disrupted by the presence of lithium nitrate ($LiNO_3$) salt. The reduction in the polycationic polyurethane

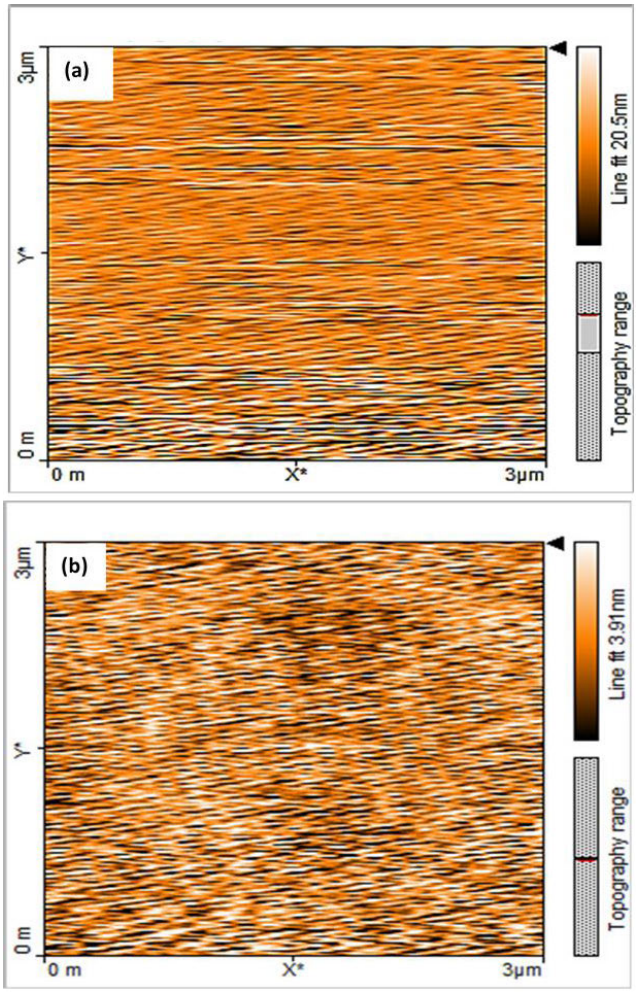

FIGURE 6. AFM images for (a) polycationic polyurethane and (b) the polycationic polyurethane thin film immersed in nitrate.

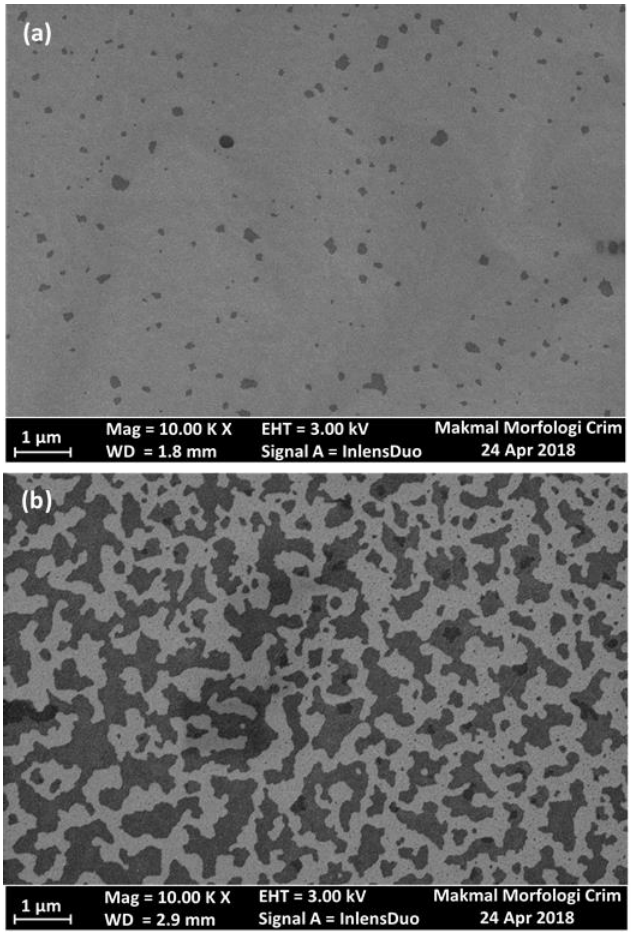

FIGURE 7. FESEM images for (a) polycationic polyurethane and (b) polycationic polyurethane-nitrate.

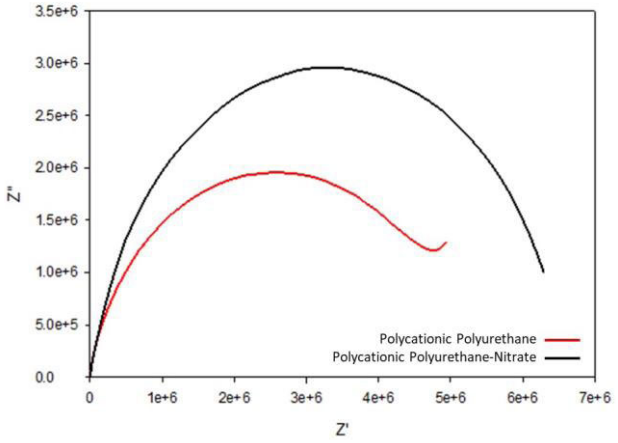

FIGURE 8. Nyquist plot (a) polycationic polyurethane and (b) polycationic polyurethane-nitrate.

crystallinity occurs due to the separation of both segments from their molecular chain to another chain of polycationic polyurethane and may also occur due to the ion exchange between the iodide and nitrate ions. The hard segment of polycationic polyurethane consists of isocyanate functional groups, where the negatively charged nitrate ion is crosslinked with the positively charged nitrogen atom of the isocyanate functional group. Hence, softer segments are produced in the structure.

D. ELECTROCHEMICAL IMPEDANCE SPECTROSCOPY (EIS)

EIS analysis was performed using film-coated fluorine-doped tin oxide (FTO) as the symmetrical conductive electrode to study the electrical properties of polycationic polyurethane and polycationic polyurethane-nitrate. The analysis was repeated three times to get an average reading. Figure 8 shows the Nyquist spectra for (a) polycationic polyurethane and (b) polycationic polyurethane-nitrate plotted using ZSimDemo 3.40d software. Polycationic polyurethane-nitrate shows higher resistivity (5.699×10^6 Ωcm) in comparison to that of polycationic polyurethane (3.303×10^6 Ωcm). A high ionic conductivity reflects the number of mobile ions in the sensing materials. Table 2 shows summaries of the resistivity and conductivity of polycationic polyurethane and polycationic polyurethane-nitrate.

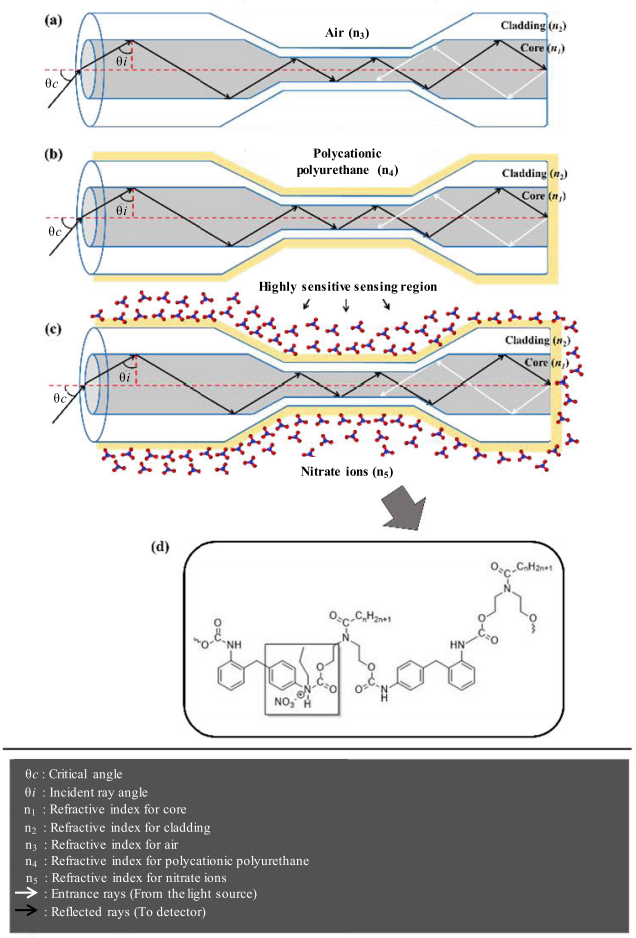

FIGURE 9. Schematic diagram of the nitrate-sensing mechanism for the proposed tapered optical fiber sensor in the (a) bare tapered optical fiber, (b) tapered optical fiber coated with polycationic polyurethane, (c) presence of nitrate on the surface of the tapered optical fiber coated with polycationic polyurethane and (d) molecular interaction of nitrate on the surface of polycationic polyurethane during the sorption process.

E. SENSING MECHANISM

Light that propagates along the optical fiber core undergoes total internal reflection at the interface between the two media with different refractive indices, namely, the core and cladding [22]. Due to this phenomenon, a strong evanescent field exists near the core-cladding interface and interacts with the chemical analytes. However, the typical core-cladding diameter of the optical fiber limits the interaction between the evanescent field and the chemical analyte outside the fiber. To improve this limitation, the fiber is tapered to thin down the core-cladding diameter, enhancing the interaction between the evanescent field and the chemical analytes [10].

In Figure 9(a), the light propagates along the optical fiber core and interacts with the chemical analytes on the surface of the tapered region of the optical fiber. Upon reaching the end of the fiber, the light is reflected following the Fresnel law of reflection and produces a measurable signal. Meanwhile, in Figure 9(b) and 9(c), the same principle applies, however, there is interaction between the light-sensing materials and the chemical analytes. A variable signal that can be measured is produced due to the refractive index differences [10]. Figure 9(d) shows the proposed chemical interaction that occurs between the sensing material and the chemical analyte on the optical fiber surface.

TABLE 2. Resistivity and conductivity of polycationic polyurethane and polycationic polyurethane-nitrate.

Sample	Resistivity (Ωcm)	Conductivity (Scm^{-1})
Polycationic Polyurethane-Nitrate	5.699×10^6	2.838×10^{-11}
Polycationic Polyurethane	3.303×10^6	5.337×10^{-11}

F. OPTICAL FIBER MORPHOLOGY

Figure 10 shows the cross-sectional images for (a) bare optical fiber, (b) optical fiber coated with polycationic polyurethane and (c) optical fiber coated with polycationic polyurethane-nitrate at 5000× magnification using an FESEM LEVO 1450VP. Figure 10(b) shows that polycationic polyurethane has been successfully coated on the optical fiber surface due to the hard segment of the polycationic polyurethane that acted as a stabilizer during the dip-coating process [17]. In Figure 10(b), a rough surface morphology is observed after polycationic polyurethane is coated on the optical fiber surface, which is also verified by the AFM analysis in Figure 6. Meanwhile, after polycationic polyurethane is immersed in nitrate solution, a smooth surface morphology is observed indicating that the chemical interaction occurs between polycationic polyurethane and nitrate as seen in Figure 10(c). The coating thickness on the optical fiber surface is 454.5 nm as shown by FESEM analysis in Figure 10(c). The dip-coater machine speed rate was fixed at 200 mm/min where it was optimized during the UV-Visible spectrophotometry study as shown in supplementary material, Figure S3.

G. RESPONSE TIME

Response time is the time taken for sensing material to sense the chemical analyte after the sensor probe is exposed to the nitrate solution. Meanwhile, recovery time is the time taken for a sensor to reach the baseline again when the sensor probe is exposed to deionized water immediately after being exposed to nitrate solution. Low response time indicates rapid interaction between the sensing material and the nitrate; hence, good sensitivity is obtained for the sensor probe. In Figure 11, the optical power decreases drastically from 93.3 a.u. to 3.3 a.u. after the sensor probe coated with polycationic polyurethane is exposed to the nitrate solution for 10 s indicating there is interaction occurring between the polycationic polyurethane and nitrate ions. However, the power output shows a constant value after 12 s due to the saturation of the adsorption site on the surface of the polycationic polyurethane; therefore, no further interaction occurs between the polycationic polyurethane and nitrate. When the sensor probe is removed from the nitrate solution, the power output increases back to 93.5 a.u. The response time at t_{90}

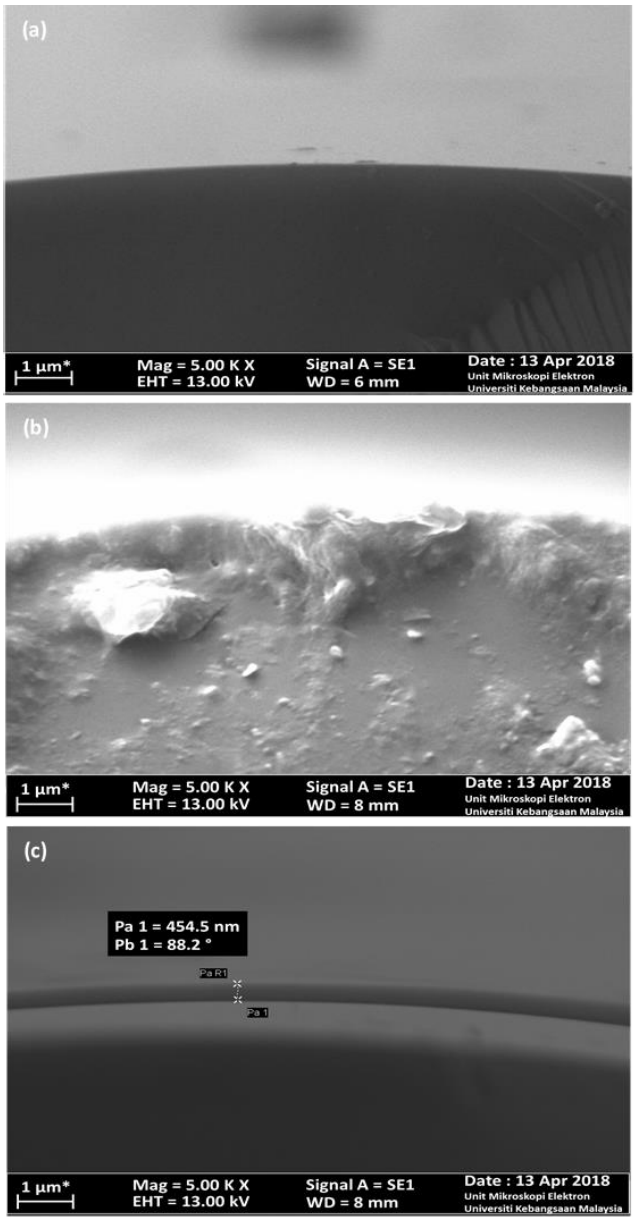

FIGURE 10. Cross-sectional SEM images for (a) the bare optical fiber, (b) the optical fiber coated with polycationic polyurethane and (c) the optical fiber coated with polycationic polyurethane-nitrate.

between the transition is 2 s, as shown in Figure 11, and the sensor probe takes 2 s to recover to its original state after it is exposed to deionized water.

H. SENSOR RESPONSE

Figure 12 shows the sensor response for (a) the bare tapered optical fiber and (b) the tapered optical fiber coated with polycationic polyurethane for nitrate sensing. As seen in Figure 12(a), when the bare tapered optical fiber is exposed to the different concentration of nitrate solutions ranging from 0 to 30 ppm, the power output increases from 0 to 1.6 μW. However, as the nitrate concentration increases, the power output does not show any significant difference between one

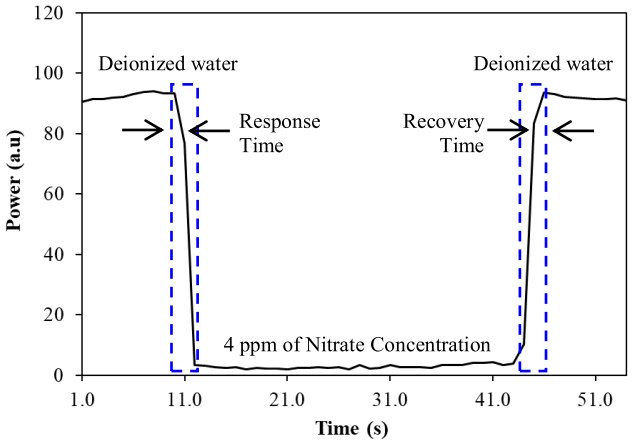

FIGURE 11. Response and recovery times for nitrate sensing using the tapered optical fiber coated with polycationic polyurethane as the sensing probe.

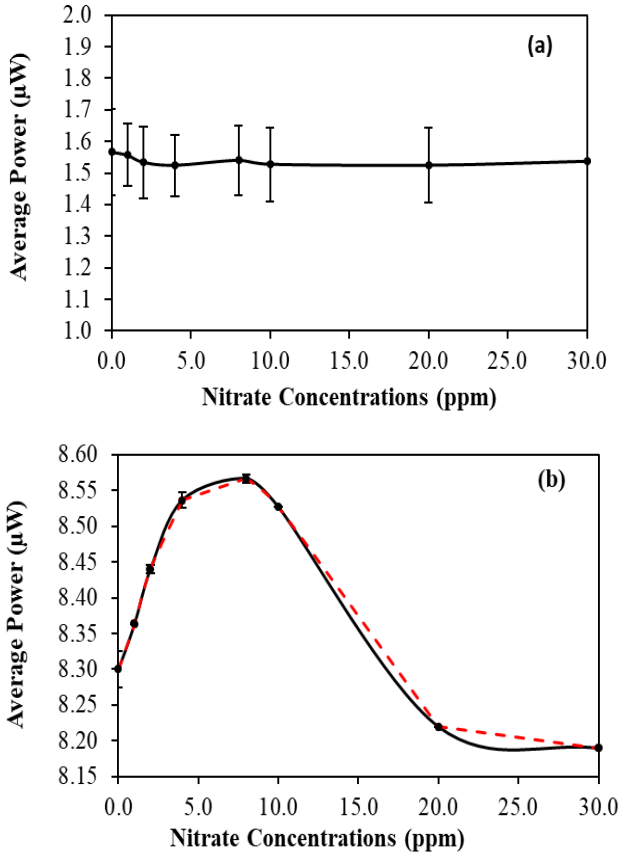

FIGURE 12. Sensor response for (a) the bare tapered optical fiber and (b) the tapered optical fiber coated with polycationic polyurethane for nitrate sensing.

another because the adsorption site on the surface of the bare tapered optical fiber is saturated. With the integration of the sensing material in Figure 12(b), more adsorption sites are available for nitrate ions that are provided by the specific functional groups of polycationic polyurethane. Therefore, a significant power output is observed between different nitrate concentrations ranging from 0 to 30 ppm. As the

concentration increases from 0 to 4 ppm nitrate concentration, the power output also increases from 8.30 μW to 8.54 μW. At this stage, the ion exchange between nitrate and iodide is rapid due to the plenty of adsorption sites available on the surface of the sensing material with a sensitivity of 5.94 $\times$ $10^{-2}\mu$W/ppm. When the sensor probe is exposed to a concentration ranging from 4.0 to 10.0 ppm, the graph shows a state of saturation due to the fully occupied adsorption sites on the surface of the sensing material [10], [21]. However, the graph starts to decline after 10.0 ppm of nitrate concentration; this is due to the higher concentration of the adsorbed analyte on the sensing material surface, thus leading to the decline in sensor sensitivity [23]. At this point, the sensor probe is no longer sensitive toward nitrate ions. The insertion loss induced by the polycationic polyurethane coating is 6.733 μW. However, the insertion loss due to the polycationic polyurethane coating is less crucial since this work used reflectance technique, instead of absorbance to measure the variation signal.

I. REPEATABILITY OF THE SENSORS

Figure 13 shows the repeatability of the nitrate sensor using the tapered optical fiber coated with polycationic polyurethane sensor probe. When the sensor probe is immersed in a 4-ppm nitrate solution during the first cycle, the power decreases from 85.5 a.u. to 1.8 a.u. When the sensor probe is exposed to air, the power increases from 1.8 a.u. to 87.5 a.u. to reach the original baseline again. The difference in power is due to the change in the refractive index during the cycle. The cycle is repeated 7 times to observe the repeatability of the sensor probe towards nitrate ion detection. Figure 13 shows that when the sensor probe is exposed to air, the graph does not recover to the approximately original baseline because of the presence of nitrate traces on the sensing material surface. However, the difference between the responses towards nitrate during the 7 cycles is slight, hence, showing the good repeatability of the sensors.

J. SELECTIVITY OF THE SENSORS

The selectivity assessment was evaluated to study the affinity of the sensing materials towards the target analyte [24]. The selectivity study was carried out by exposing the sensor probe coated with polycationic polyurethane to several other solutions that separately contained different anions, such as sulfate (SO_4^{2-}), hydroxide (OH^-) and acetate (CH_3COO^-), to study the possible interference from other anions. The solutions were prepared with different concentrations ranging from 0 to 30 ppm. Figure 14(a) illustrates that the sensor probe shows good selectivity toward nitrate ions in comparison to other anions, which can be observed based on the large difference in power response for nitrate (>8.0 μW) compared to that for the other interfering anions. This result is due to the hydrophobic nature of the sensing material, hence, suggesting that the polycationic polyurethane possesses high affinity toward the nitrate ion [25]. The effect of the interference from a cation was also investigated. Figure 14(b) depicts that the

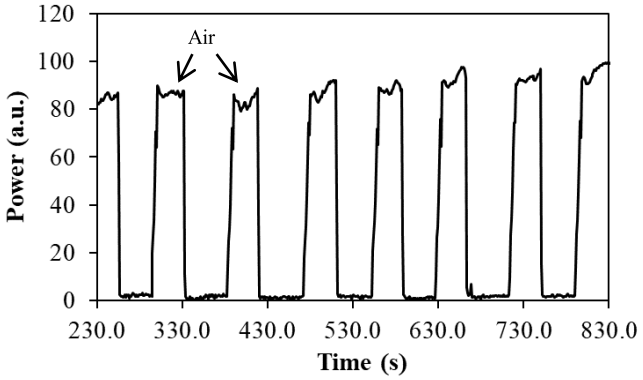

FIGURE 13. Repeatability for the sensing probe coated with polycationic polyurethane.

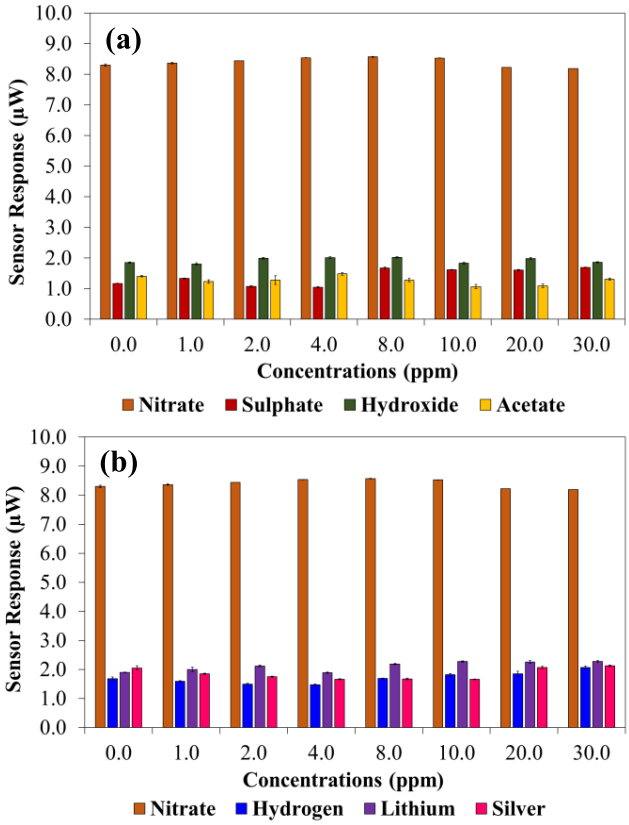

FIGURE 14. Interference study for the sensing probe coated with polycationic polyurethane toward (a) anions and (b) cations.

polycationic polyurethane shows low affinity toward cations in comparison to that of the nitrate ion.

IV. CONCLUSION

A tapered optical fiber coated with a bio-based polycationic polyurethane as a sensor probe for nitrate sensing was successfully fabricated for rapid detection with a sensitivity of 5.94 $\times$ $10^{-2}\mu$W/ppm. The intermolecular interaction at active polymeric sites played a primary role in selective-ion detection. The occurrence of nitrate detection on the polycationic polyurethane surface was verified by FTIR, AFM and FESEM analyses. Good selectivity was also observed for

the sensor, indicating that polycationic polyurethane had high affinity toward the nitrate ion.

ACKNOWLEDGMENT

The authors are grateful to the Photonics Technology Laboratory, Center of Advanced Electronic and Communication Engineering (PAKET); the Faculty of Engineering and Built Environment, Solar Energy Research Institute (SERI); and the Center for Research and Instrumentation Management (CRIM), Universiti Kebangsaan Malaysia (UKM), for all the facilities provided.

REFERENCES

[1] J. L. Camas-Anzueto, A. E. Aguilar-Castillejos, J. H. Castañón-González, M. C. Lujpá-Hidalgo, H. R. H. de León, and R. M. Grajales, "Fiber sensor based on Lophine sensitive layer for nitrate detection in drinking water," *Opt. Lasers Eng.*, vol. 60, pp. 38–43, Sep. 2014.

[2] M. Y. Chong, M. Z. M. Jafri, L. H. San, and T. C. Ho, "Detection of nitrate ions in water by optical fiber," in *Proc. Int. Conf. Comput. Commun. Eng.*, Kuala Lumpur, Malaysia, Jul. 2012, pp. 271–273.

[3] N. Öztürk and T. E. Bektaş, "Nitrate removal from aqueous solution by adsorption onto various materials," *J. Hazardous Mater.*, vol. 112, nos. 1–2, pp. 155–162, 2004.

[4] G. A. Crespo, "Recent Advances in Ion-selective membrane electrodes for in situ environmental water analysis," *Electrochim. Acta*, vol. 245, pp. 1023–1034, Aug. 2017.

[5] C. Lopez-Moreno, I. V. Perez, and A. M. Urbano, "Development and validation of an ionic chromatography method for the determination of nitrate, nitrite and chloride in meat," *Food Chem.*, vol. 194, pp. 687–694, Mar. 2016.

[6] M. R. Siddiqui, S. M. Wabaidur, Z. A. AlOthman, and M. Z. A. Rafiquee, "Rapid and sensitive method for analysis of nitrate in meat samples using ultra performance liquid chromatography–mass spectrometry," *Spectrochim. Acta A, Mol. Biomol. Spectrosc.*, vol. 151, pp. 861–866, Dec. 2015.

[7] Y. C. Moo, M. Z. Matjafri, H. S. Lim, and C. H. Tan, "New development of optical fibre sensor for determination of nitrate and nitrite in water," *Optik*, vol. 127, no. 3, pp. 1312–1319, 2016.

[8] A. S. Lalasangi, J. F. Akki, K. G. Manohar, T. Srinivas, P. Radhakrishnan, S. Kher, N. S. Mehla, and U. S. Raikar, "Fiber Bragg grating sensor for detection of nitrate concentration in water," *Sensors Transducers J.*, vol. 125, no. 2, pp. 187–193, 2011.

[9] S. Idris, N. H. Azeman, N. A. N. Azmy, C. T. Ratnam, M. A. Mahdi, and A. A. A. Bakar, "Gamma irradiated Py/PVA for GOx immobilization on tapered optical fiber for glucose biosensing," *Sens. Actuators B, Chem.*, vol. 273, pp. 1404–1412, Nov. 2018.

[10] W. B. W. A. Rahman, N. H. Azeman, N. H. Kamaruddin, P. S. Menon, A. A. Shabaneh, M. A. Mahdi, M. H. H. Mokhtar, N. Arsad, and A. A. A. Bakar, "Label-free detection of dissolved carbon dioxide utilizing multimode tapered optical fiber coated zinc oxide nanorice," *IEEE Access*, vol. 7, pp. 4538–4545, 2019.

[11] L. Liu, X. Wu, and T. Li, "Novel polymer electrolytes based on cationic polyurethane with different alkyl chain length," *J. Power Sources*, vol. 249, pp. 397–404, Mar. 2014.

[12] S. Wang and K. Min, "Solid polymer electrolytes of blends of polyurethane and polyether modified polysiloxane and their ionic conductivity," *Polymer*, vol. 51, no. 12, pp. 2621–2628, 2010.

[13] F. Jasmi, N. H. Azeman, A. A. A. Bakar, M. S. D. Zan, K. H. Badri, and M. S. Su'ait, "Ionic conductive polyurethane-graphene nanocomposite for performance enhancement of optical fiber Bragg grating temperature sensor," *IEEE Access*, vol. 6, pp. 47355–47363, 2018.

[14] H. Liu, J. Gao, W. Huang, K. Dai, G. Zheng, C. Liu, C. Shen, X. Yan, J. Guo, and Z. Guo, "Electrically conductive strain sensing polyurethane nanocomposites with synergistic carbon nanotubes and graphene bifillers," *Nanoscale*, vol. 8, no. 26, pp. 12977–12989, 2016.

[15] Y. He, W. Li, G. Yang, H. Liu, J. Lu, T. Zheng, and X. Li, "A novel method for fabricating wearable, piezoresistive, and pressure sensors based on modified-graphite/polyurethane composite films," *Materials*, vol. 10, no. 7, p. 684, 2017.

[16] K. H. Badri, S. H. Ahmad, and S. Zakaria, "Development of zero ODP rigid polyurethane foam from RBD palm kernel oil," *J. Mater. Sci. Lett.*, vol. 19, no. 15, pp. 1355–1356, 2000.

[17] M. S. Su'ait, A. Ahmad, K. H. Badri, N. S. Mohamed, M. Y. A. Rahman, C. L. A. Ricardo, and P. Scardi, "The potential of polyurethane bio-based solid polymer electrolyte for photoelectrochemical cell application," *Int. J. Hydrogen Energy*, vol. 39, no. 6, pp. 3005–3017, 2014.

[18] M. S. Su'ait, N. N. Mobarak, M. Faizal, K. H. Badri, and A. Ahmad, "Novel bio-based polyurethane polycation for solid-state electrochemical devices application," in *Proc. 15th Int. Symp. Polym. Electrolytes*, Uppsala, Sweden, Aug. 2016, p. 84.

[19] E. C. Buruiana and T. Buruiana, "Synthesis and characterization of novel polyurethane cationomers with dipeptide sequences and alkylammonium groups," *J. Biomater. Sci.*, vol. 15, no. 6, pp. 781–795, 2004.

[20] H. Sakamoto, H. Asakawa, T. Fukuma, S. Fujita, and S. Suye, "Atomic force microscopy visualization of hard segment alignment in stretched polyurethane nanofibers prepared by electrospinning," *Sci. Technol. Adv. Mater.*, vol. 15, no. 1, 2014, Art. no. 015008.

[21] S. Abdullah, N. H. Azeman, N. N. Mobarak, M. S. D. Zan, and A. A. A. Bakar, "Sensitivity enhancement of localized SPR sensor towards Pb(II) ion detection using natural bio-polymer based carrageenan," *Optik*, vol. 168, pp. 784–793, Sep. 2018.

[22] R. Orghici, U. Willer, M. Gierszewska, S. R. Waldvogel, and S. Schade, "Fiber optic evanescent field sensor for detection of explosives and CO_2 dissolved in water," *Appl. Phys. B, Lasers Opt.*, vol. 90, no. 2, pp. 355–360, 2008.

[23] M. Ermel, R. Oswald, J.-C. Mayer, A. Moravek, G. Song, M. Beck, F. X. Meixner, and I. Trebs, "Preparation methods to optimize the performance of sensor discs for fast chemiluminescence ozone analyzers," *Environ. Sci. Technol.*, vol. 47, no. 4, pp. 1930–1936, 2013.

[24] N. H. Kamaruddin, A. A. A. Bakar, N. N. Mobarak, M. S. D. Zan, and N. Arsad, "Binding affinity of a highly sensitive Au/Ag/Au/chitosan-graphene oxide sensor based on direct detection of Pb^{2+} and Hg^{2+} ions," *Sensors*, vol. 17, no. 10, p. 2277, 2017.

[25] T. Kikhavani, S. N. Ashrafizadeh, and B. Van der Bruggen, "Nitrate selectivity and transport properties of a novel anion exchange membrane in electrodialysis," *Electrochim. Acta*, vol. 144, pp. 341–351, Oct. 2014.

[26] J. M. Corres, F. J. Arregui, and I. R. Matías, "Sensitivity optimization of tapered optical fiber humidity sensors by means of tuning the thickness of nanostructured sensitive coatings," *Sens. Actuators B, Chem.*, vol. 122, no. 2, pp. 442–449, 2007.

[27] A. S. Abed, K. M. Ziadan, and A. Q. Abdullah, "Some optical properties of polyurethane," *Iraqi J. Polym.*, vol. 17, no. 1, pp. 18–28, 2014.

[28] A. A. Shabaneh, S. H. Girei, P. T. Arasu, S. A. Rashid, Z. Yunusa, M. A. Mahdi, S. Paiman, M. Z. Ahmad, and M. H. Yaacob, "Reflectance response of optical fiber coated with carbon nanotubes for aqueous ethanol sensing," *IEEE Photon. J.*, vol. 6, no. 6, Dec. 2014, Art. no. 6802910.

ATIQAH YUSOFF received the B.Sc. degree (Hons.) in microelectronic engineering from Universiti Kebangsaan Malaysia, in 2018. During her final year project, she was involved in development of multimode optical fiber sensors based on polyurethane polycation as the sensing material for detection of nitrate ion in water. She is currently a Test Engineer with ViE Technologies Sdn. Bhd.

NUR HIDAYAH AZEMAN received the B.Sc. degree in resource chemistry from Universiti Malaysia Sarawak, in 2009, and the master's degree in environment and the Ph.D. degree in smart sensing materials from Universiti Putra Malaysia, in 2012 and 2017, respectively. She is currently a Postdoctoral Researcher with the Photonics Technology Laboratory, Center of Advanced Electronic and Communication Engineering (PAKET), Faculty of Engineering and Built Environment, Universiti Kebangsaan Malaysia, and her project focusing on the designing and synthesizing the sensing materials for the optical sensors application. Her research interests include functional materials, optical sensors and its applications. She is also a Registered Professional Chemist with the Malaysian Institute of Chemistry (ChM).

MUHAMMAD FAIZAL MOHAMED KASSIM received the B.Sc. degree (Hons.) in chemistry from Universiti Kebangsaan Malaysia, in 2016, where he is currently pursuing the M.Sc. degree in chemistry.

NADHRATUN NAIIM MOBARAK received the B.Sc., M.Sc., and Ph.D. degrees in chemistry from Universiti Kebangsaan Malaysia (UKM), Malaysia, in 2008, 2011, and 2015, respectively. She is currently a Senior Lecturer with the Center for Advanced Materials and Renewable Resources (CAMARR), Faculty of Science and Technology, Universiti Kebangsaan Malaysia. Her research interests include the functional biomaterial, water adsorbent and energy conversion and storage devices.

KHAIRIAH HAJI BADRI received the bachelor's degree in chemistry and the B.E. degree in chemical and petroleum refining engineering from the Colorado School of Mines, USA, in 1993, and the Ph.D. degree in material sciences with a focus on polymer synthesis and technology. She is currently a Professor with the Faculty of Science and Technology, School of Chemical Sciences and Food Technology, Universiti Kebangsaan Malaysia. She is also the Head of the Polymer Research Center, pioneering in thermosetting polymers from natural resources, such as palm oil, coconut oil, soybean oil, and agricultural biomass and converts them to polyurethanes. She is also intensively running a precommercialization project on the utilization of palm kernel oil and converted to polyol.

MOHD ADZIR MAHDI (M'99–SM'03) received the B.Eng. degree from Universiti Kebangsaan Malaysia, in 1996, and the M.Sc. and Ph.D. degrees from the University of Malaya, in 1999 and 2002, respectively. He is currently a Professor with the Wireless and Photonics Network Research Center, Faculty of Engineering, Universiti Putra Malaysia. His research interests include photonic devices and optical communication.

MOHD SUKOR SU'AIT received the B.Sc., M.Sc., and Ph.D. degrees in chemistry from Universiti Kebangsaan Malaysia (UKM), Malaysia, in 2007, 2010, and 2014, respectively. He is currently a Research Fellow with the Solar Energy Research Institute and an Associate Researcher with the Polymer Research Center, UKM. He had published about 15 articles in international refereed journal with an H-index, 5. His research interest includes electrochemistry covers the synthesis and characterization of electrochemical materials for energy storage and conversion devices (lithium batteries and solar cell). In 2009, he has been selected as a Young Scientist to represent The Association of Southeast Asian Nations (ASEAN), in the 59th Nobel Laureates Meeting, dedicated to chemistry at Lindau, Germany, and honored as an ASEAN Scientist for Tomorrow by ASEAN at Jakarta, Indonesia, in 2009. He was a recipient of the Erasmus Mundus Mobility Program, University of Trento, Italy, in 2011, the Attachment Program at the Georgia Institute of Technology, USA, in 2012, and Cadi Ayyad University, Morocco, in 2014.

AHMAD ASHRIF A. BAKAR (M'02–SM'12) received the bachelor's degree in electrical and electronics engineering from Universiti Tenaga Nasional, in 2002, the M.Sc. degree in communications and network system engineering from Universiti Putra Malaysia, in 2004, and the Ph.D. degree in electrical engineering from The University of Queensland, Australia, in 2010. He is currently an Associate Professor with the Center of Advanced Electronic and Communication Engineering (PAKET), Faculty of Engineering and Built Environment, Universiti Kebangsaan Malaysia. He is actively involved in the Optical Society of America and Fiber Optic Association Inc., USA. He is devoting his research work on optical sensors in environmental and biomedical applications, specialized in plasmonic waveguide sensor, polymeric electro-optic modulator waveguide, interferometer, evanescent field sensors, and devices based on nanoparticles and nanostructures. He has been a member of OSA, since 2014.